Journal of Data Acquisition and Processing
ISSN: 1004-9037
https://sjcjycl.cn/
DOI: 10.5281/zenodo.777179

AD-TL: ALZHEIMER'S DISEASE PREDICTION USING TRANSFER LEARNING

Archana Gopinadhan
Research Scholar, Department of Computer Science, AJK College of Arts and Science, Coimbatore- 641 105.

Dr. Angeline Prasanna G
Former Associate Professor and Head, Department of Computer Science, AJK College of Arts and Science, Coimbatore- 641 105.

Abstract

Differentiating Alzheimer's and healthy brain data in older adults (age > 75) has proven challenging due to highly similar patterns of brain atrophy and image intensities, even though numerous statistical methods and machine learning algorithms have been investigated in both clinical and research settings to extract these patterns from neuroimaging data. Medical image analysis is just one field that has benefited from the widespread use of deep learning technologies in recent years. This research paper proposed AD prediction using transfer learning (AD-TL) methods. The MRI dataset has been normalized using the Multi-Layer Perception model (MLP) with the CNN algorithm. The Image enhancement has been utilized with the Contrast Limited Adaptive histogram equalization CLAHE method. Image segmentation has been done with Watershed Image segmentation. The training has been done with the Residual network (ResNet 50) with Alex net. Finally, the classification has been done with the Deep Convolutional neural network (DCNN) algorithm. According to the experimental data, the classification accuracy of the technique provided in this study may reach 99%.

Keywords: Alzheimer's disease, CNN, DCNN, MRI, ResNet, Watershed, Prediction

I INTRODUCTION

Alzheimer's disease (AD) is a multi-factorial, irreversible [1], degenerative neurological brain condition that gradually destroys brain cells, resulting in memory and cognitive impairment and, finally, the inability to perform even the most fundamental functions [2]. Due to the long-term effects on cognition, this condition is a leading cause of dementia [3]. This gradual decline over time is characteristic of neurodegenerative dementia [4]. Diagnosing Alzheimer's disease requires a thorough evaluation of the patient's medical history, a short mental state examination (MMSE), and physical and neurological testing. Brain morphology, functional brain activity, and alterations may also be evaluated non-invasively using structural magnetic resonance imaging (sMRI) and resting-state functional magnetic resonance imaging (rs-fMRI) [6]. Patients must lie prone on the MRI table and not move throughout structural (anatomical) and rs-fMRI scans [7]. [8-12]. This allows data collection to continue independent of the influence of a given task on functional brain activity. Alzheimer's disease shrinks the hippocampus and cerebral cortex while expanding the brain's ventricles [13]. The degree of these consequences is influenced by the stage of the disease's development. MR images of

individuals with severe Alzheimer's disease show substantial hippocampal and cerebral cortical atrophy and considerable ventricular enlargement [14]. The areas and connections in the brain responsible for reasoning, remembering (particularly short-term memory), planning, and judging are all negatively impacted. Wounded areas of the brain have reduced MR image (or signal) intensities in MRI and rs-fMRI due to the death of nearby brain cells.

Nonetheless, a number of the signals identified in AD imaging data are also present in data from the general population as they age. Accurate data classification demands extensive knowledge and ability when differentiating between data related to Alzheimer's disease (AD) and photos of older adults showing usual ageing indications (i.e. MMSE). Clinicians have been looking for a way to classify MR-based imaging data (including structural MRI and rs-fMRI data) and, more significantly, to separate data from patients with brain diseases from data from healthy individuals. Researchers and doctors will be aided in their quest to find a cure for Alzheimer's by the robust machine learning algorithm known as Deep Learning, which can detect brain illness.

This paper's primary contributions are as follows:

- MRI image normalization using MLP with CNN algorithm
- Image enhancement using CLAHE with histogram equalization
- Image segmentation has been done with watershed segmentation
- The dataset has been trained with RESNet50 with AlexNet architecture
- AD Multi-class classification using D-CNN algorithm.

Section 2 of this research will go through the methods currently used to diagnose AD. The AD-TL model is shown in Figure 3. The results and discussion of the AD-TL model are presented in Section 4. Conclusions and suggestions for further research are presented in Section 5.

II BACKGROUND STUDY

A. Raj et al. [1] In this study, the author proposes a new CNN architecture with efficientNetV2 for Alzheimer's disease diagnosis, one that uses a Change process that has shown to be effective for analyzing large sets of images. The proposed system was created to focus on internal resource use. On a subset of four people from the ADNI database, the classification performance of AD/CNN and AD/CNN+EfficientNetV2 was 1.0 and 0.95, respectively. We may learn how to process more frames per second in the future. There is room for improvement in the structural approach of the suggested method that would reduce the amount of time and effort required to produce the model.

B. Shi et al. [3] This article proposes a DIML approach to the AD staging issue. This author's solution was novel because it extends the binary class-equivalent or inequivalent limitations of previous metric learning algorithms to permit varying degrees of similarity across data points. These similarities were then recorded as a pairwise distance matrix, with the distances between ADNI patients represented by the difference between their group-wise MMSE scores. Future work would focus on incorporating new domain data and researching other features.

C. A. Ortiz Toro et al. [5] The outcomes of this research suggest that specific radiometric characteristics (e.g., LAHGLE) might be used as biomarkers to detect Alzheimer's

disease. Like in previous studies, the hippocampus and amygdala were shown to be the most significant locations for MRI AD/CN differentiation. Considering the overall performance measures for the various characteristics, this study demonstrates that Neuromorphometrics and Hammers had a little edge over the other atlases for Alzheimer's disease identification, even though performance differences were often tiny.

M. Mahyoub et al. [8] Briefly, this work aimed to analyze the ADNI dataset, not to assert that any conclusions drawn from that analysis had any clinical significance. Data from the Alzheimer's Disease Neuroimaging Initiative, from which this research was developed, were utilized (ADNI). We gathered data on potential risk factors for Alzheimer's disease from respondents while protecting their anonymity. Biological risk factors include medical history, genetics, and symptoms of illness, whereas behavioural risk factors include things like one's way of life, one's demographics, and one's qualities.

Q. Zhou et al. [10] When trying to detect Alzheimer's disease and mild cognitive impairment, performing a battery of tests was crucial. When used with the MMSE, data from volumetric MRI scans may improve AD prediction (aMCI or naMCI). The MMSE score was the most statistically significant variable throughout the AD spectrum, contributing to an increased classification accuracy of almost 10%. When the MMSE score was used with MRI measures of the right hippocampus and the left inferior lateral ventricle to identify AD patients from CN, a classification accuracy of 92.4% (sensitivity: 84.0%; specificity: 96.0%) was reached. The findings were extremely close to those found in other recent research, indicating that the strategy explored for choosing and subsequently grading MMSE and other MRI characteristics may enhance other classification systems found in the literature. This may become more significant when AD prognostic criteria are reevaluated.

Rapaka, D et al. [12] Microglia's detrimental production of inflammatory cytokines after activation may be mitigated by drugs that target cannabinoid and cannabinoid-like receptors. Investment in creating high-quality preclinical neuroinflammation models of Alzheimer's disease is essential. There was a need for a study to minimize microglial aggregation at fibril sites and to mitigate the psychotropic adverse effects of cannabis medicines—the alteration of essential microglial activation pathways by cannabinoids and cannabinoid-like drugs. Because cannabis' pharmacological actions do not correspond with currently available drugs, the author feels that this research area may be more beneficial for treating neuroinflammation and may lead to innovative therapeutic agents for Alzheimer's disease. As a result, understanding the pharmacology of cannabis in microglial cells was critical to creating a new and more effective therapy for Alzheimer's disease (AD) patients and slowing the disease at the cellular/preclinical stage.

III MATERIALS AND METHODS

The proposed model is named the AD-TL method for early AD prediction. This AD-TL method has utilized MLP for noise removal, and hybrid deep learning algorithm for training, and CNN for classification.

3.1: Dataset Description:

The MR image on this page may be used to build a diagram of the brain's architecture, including the medulla oblongata, emphasizing input structure. Many parts of a picture may be identified individually. The proposed work is executed on AD-related datasets obtained from

the https://www.kaggle.com/datasets/tourist55/alzheimers-dataset-4-class-of-images website link.

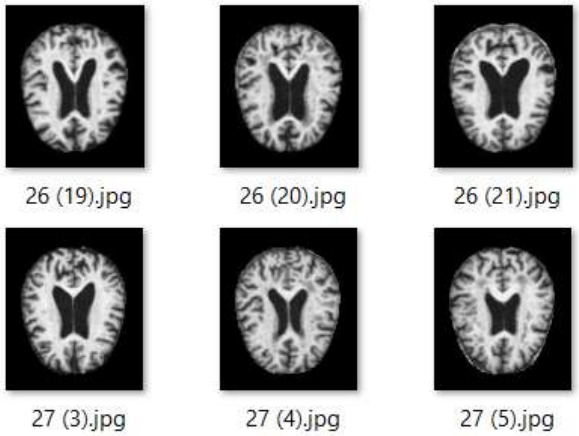

Figure 1: Sample MRI Images

3.2 Multi-Layer Perception Networks With CNN

As seen in Figure 2, multi-layer perceptual architecture consists of two intermediate "hidden" layers and an "output" layer. There are three parts to a network of this kind: the visible input layer, the hidden layer of numerous computer nodes, and the visible output layer. The input signal spreads outward in a supplementary fashion.

Using the back-propagation algorithm, multi-layer perception networks are trained for network analysis.

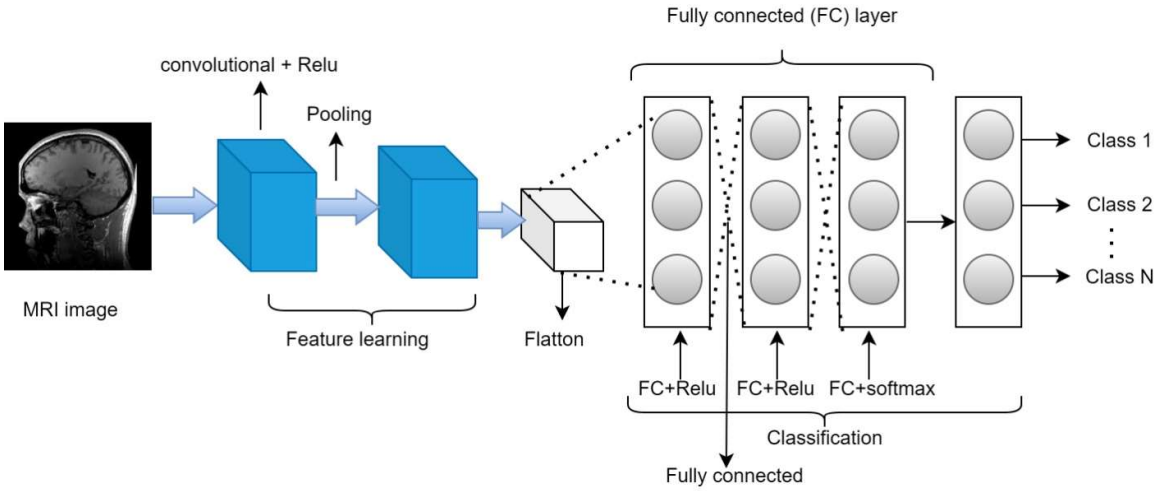

Figure 2: The construction drawing of multi-layer perception with two hidden layers

(1) Objective function Selection

The regularisation part of the network is driven by design, i.e. Bayes methods are led in neural network analysis. Assuming weight follows a Gaussian distribution, the regularisation item appears as follows:

$$R(\boldsymbol{w}) = \frac{1}{2}\sum_{j=1}^{N_w} w_j^2 \quad \text{------ (1)}$$

Crossover tests are utilized for training the network in the network training progression. After completing the specified number of iterations, test the sample set. Suppose the mean square training error is $E_T(\boldsymbol{w})$, the performance function is $\boldsymbol{C(w)}$, and performance function $C(\mathbf{w})$ is shown as formula（2）:

$$C(w) = E_T(\boldsymbol{w}) + \xi R(\mathbf{w}) \text{ --------- (2)}$$

ξ is regularising parameter.

Suppose a generalization error is $E_G(\boldsymbol{w})$, the overall error is $E(\mathbf{w})$, and overall error E(w) is shown as formula（3）

$$E(w) = \frac{C(\boldsymbol{w}) + E_G(\boldsymbol{w})}{2} \quad \text{-------- (3)}$$

The objective of this optimization issue is to minimize the combination property function E(w), and the sufficiency function is denoted by the formula: (4)

$$f(w) = \frac{1}{1+E(w)} \text{ ------- (4)}$$

3.3 Contrast Limited Adaptive Histogram Equalization

It has been shown that Contrast Limited Adaptive Histogram Equalization (CLAHE) is superior to Adaptive Histogram Equalization (AHE) [8]. CLAHE mitigates the problems caused by AHE by restricting the improvement of contrast in uniform regions. Assigning additional pixels to the same grayscale range, as shown in a histogram peak that depends on context.

To do this, CLAHE adjusts the intensity values in the image, working in tiny squares (called tiles) and using bilinear interpolation to eliminate the edges of the tile and smooth out the neighbouring pixels. Conventional histogram equalization may lead to brightness saturation. However, CLAHE considerably decreases picture noise.

In this scenario, the exponential distribution [8] will be used to spread the grey-level distribution among the pixels in the histogram, which recognizes that the pixels may have different distributions.

$$\beta = \frac{M}{N}\left(1 + \frac{a}{100}(S_{max} - 1)\right) \text{ ------ (5)}$$

Exponential:

$$g = g_{min-(1/\alpha)*} \ln[1 - \mathrm{p(f)}].$$

g_{min}= minimum pixel value

g_{max} = maximum pixel value

g = computed pixel value

α = parameter

p(f) =cpd (cumulative probability distribution

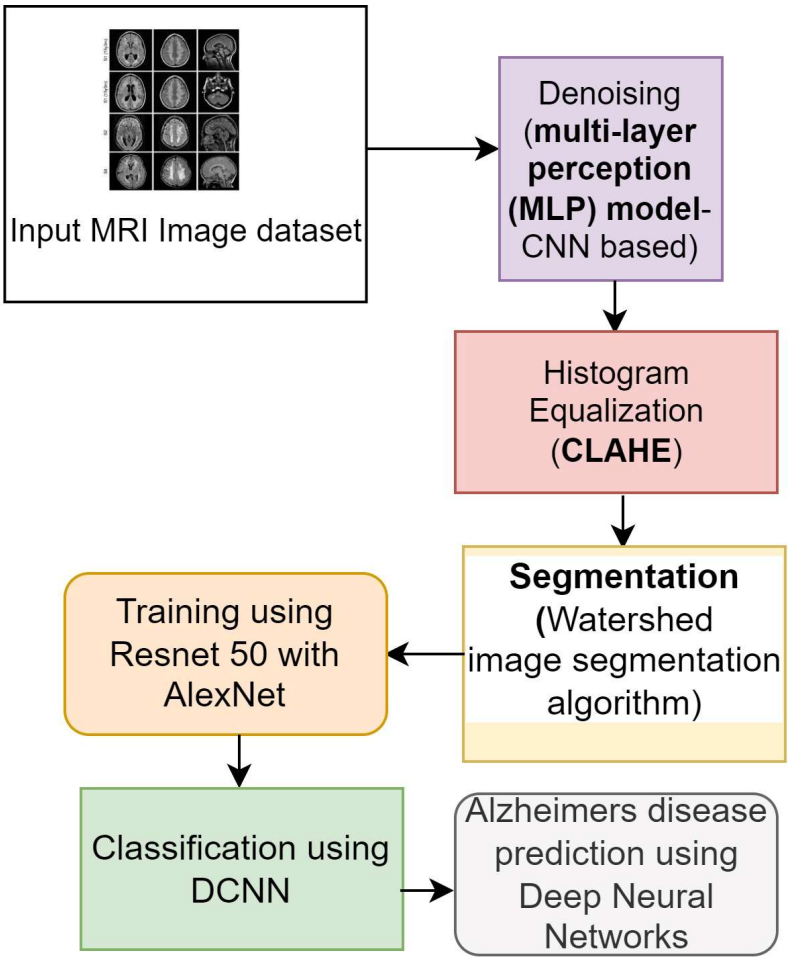

Figure 3: Architecture Diagram for AD-TL framework

3.4 Watershed image segmentation

The kernel density estimation method, commonly known as the Parzen window technique in pattern recognition, is widely used to calculate density estimates in feature space analysis. The multivariate fixed bandwidth kernel density estimate is denoted as where n is the number of data points and d is the dimension of the space in which they are located.

$f^{\Lambda}(x) = \frac{1}{nh^d}\sum_{i=1}^{n} \mathbf{K}(\frac{(x-x_i)}{h}$ -------- (6)

Where h is the constant bandwidth across the network. $x \in R^d$and $\mathbf{k}$(x) is a radically symmetric kernel

Identifying its modes is the first step in evaluating a feature space where f(x) represents the underlying density. The modes are positioned among the gradient's zeros $\nabla f(x)0$. The mean-shift strategy is the most effective method for locating these zeros without estimating the density. The mean shift vector always points in the direction of the most significant density increase.

Consider the classification of z into C classes, Z_i i=1…C. Let m_i represent the average of the N_i data points in class z_i

$\mathrm{m_i} = \frac{1}{\mathrm{N_i}} \sum_{z \in Z} z$ -------- (7)

Let $S_{T=\sum_{z \epsilon Z} \|z-m\|} 2$ and $S_w = \sum_{i=1}^{c} S_i = \sum_{i=1}^{c} \sum_{z \in z_i} \|z - m_i\|$ ---------- (8)

The definition of the dimension J is

$J = \frac{(S_T - S_W)}{S_W}$ ------- (9)

It compares the distances between members of distinct classes $(S_T - S_W)$ against those between members of the same class S_W. A more excellent value of J indicates that the classes are more apart, but the members within each class are closer together, and vice versa.

3.5 Training with ResNet-50 with AlexNet

ResNets is a design for neural networks that incorporates the Residual Learning method into its wiring. This approach prevents parameter values from being saturated by adding the Value of the shortcut, which is the single layer of the liner player linked to the network from input to output after it passes through one or more specified layers and the function F(x) (vanishing gradient).

On the assumption that a complex function may approximate the output of several nonlinear layers, Residual Learning theory draws the conclusion that such a mapping exists., means $F(x) = H(x) - x$, it can convert the formula to $H(x) = F(x) + x$, training can be accelerated and vanishing gradients avoided if we create a shortcut using x as an input to the function F(x).

To combat the vanishing gradients, ResNets made use of shortcut connections to skip over one or more levels, creating a structure known as a Residual Block. ResNets must create two separate Residual Blocks, the identity block and the convolutional block. The identifying Block of ResNets is a typical Residual Block with identical input and output sizes. By use of Residual Learning, Identity Block demonstrated Eq (10).

$\mathcal{Y} = F(x, \{W_i\}) + x$ -------- (10)

The Identity Block is shown in its original state in Figure 2. The ReLU function acts as a switch, switching the model to its nonlinear, formula-described state. Y=max (0,x) (0,x). A Convolutional Layer, the Weight Layer, and the subsequent Batch Normalization technique are used to standardize features in a zero-mean condition by a factor of 1.

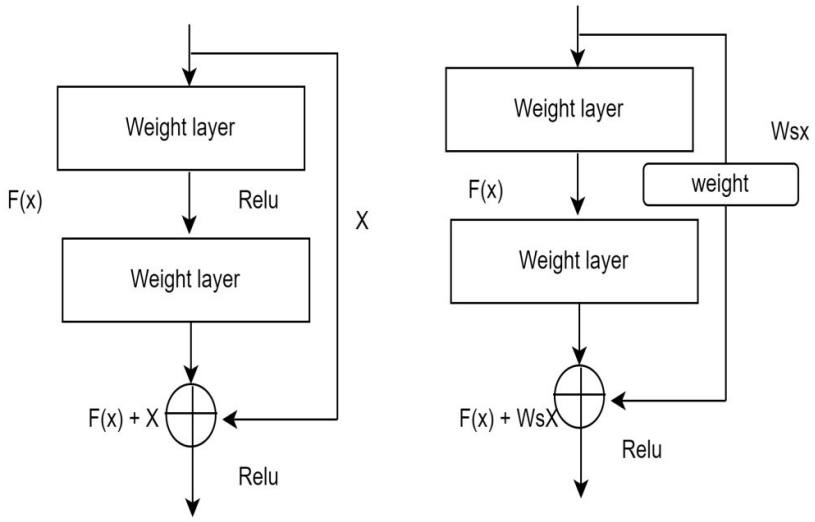

Fig 4. Original Identity Block and Convolutional Block structure.

Like the Identity Block, the Residual Block, known as the Convolutional Block, uses the Residual learning technique. In contrast, the quick cut built a Weight Layer to adjust the Value of the specified parameter. W_s. The layout is shown in Fig. 2, and the Convolutional Block's universal formula is represented by the (11).

$$\mathcal{Y} = F(x, \{W_i\}) + W_s x \text{ -------- (11)}$$

As shown in this study, reduced training times were achieved by adding a weight layer to the Identity Block and Convolutional Block model. Figure 3 depicts IdentityBlock and Convolutional Blockvariants.

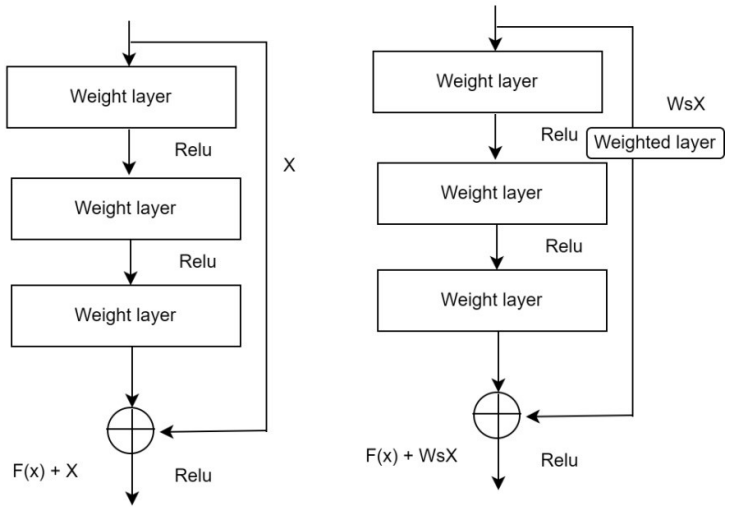

Fig. 5 Variable Identity Block and Convolutional Block structure.

The convolutional 7x7 input layer of the ResNet-50 model is shown in Figure 4. Convolutional blocks and converted identity blocks, each with three convolution layers and a shortcut link, comprise the sixteen residual blocks divided over stages 2-4-5. One convolutional block and two identity blocks, each with a block size of 64, make up Stage 2. Stage 3 block size includes one convolutional block and three identity blocks for 128. This stage's neural network consists of 1 convolutional block and 5 identity blocks, with a block size of 256. In

the fifth stage, we use a 512-by-512 block size for both the convolutional and identification blocks. To adapt the feature size to the parameters of each stage, the convolutional block is placed at the start of each phase.

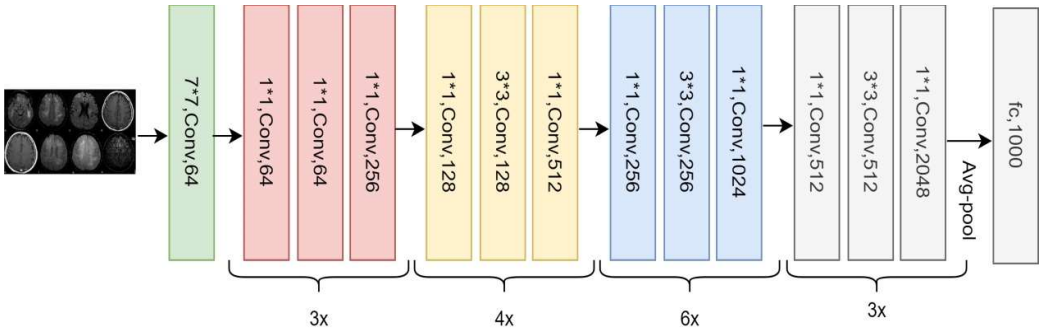

Fig. 6. Structure of the ResNet-50 A-disease recognition model.

3.5.1 Description of AlexNet

AlexNet is a well-known design for neural networks. It received widespread recognition for participating in and winning the 2012 ImageNet Large Scale Visual Recognition Challenge. The network achieves a phenomenal error rate of 15.3%, 10.8 percentage points lower than its closest competitor. AlexNet is based on the principle that model depth is crucial for performance. Therefore, it was coded in CUDA to be executed on a GPU for faster training. AlexNet is not the first network to train on GPU, but its impact in this sector is enormous. One of the most influential works in image recognition, it stimulates more research than GPU training. The standard AlexNet (Figure 5) consists of five convolutional layers, three max-pooling, and three fully linked layers.

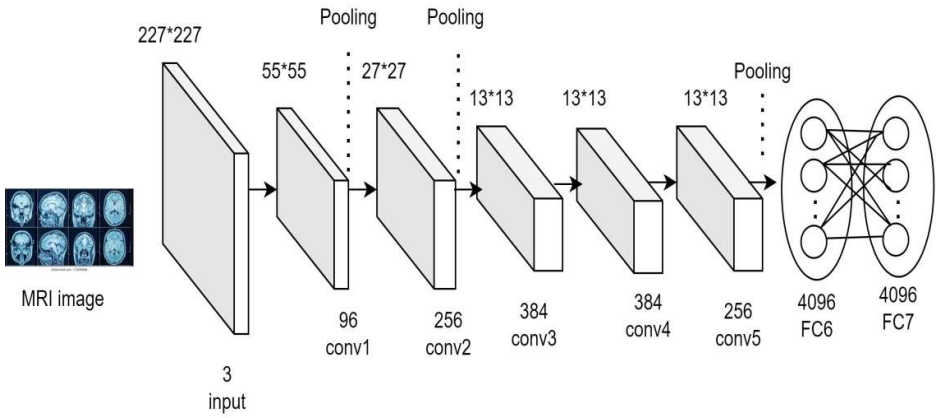

Figure 7: Alexnet architecture

3.6 Prediction using Deep ConvNet Model

Convolutional layers are the backbone of every deep CNN, and advanced activation functions allow them to perform at their peak. The suggested deep CNN (deep ConvNet) model uses a deep convolutional neural network to automatically extract data from whole-brain MRI scans for Alzheimer's disease detection. As shown in Fig. 2, the proposed model requires sliced, preprocessed 2D data as input. Each book has 500–600 individual slices, depending on the subject.

With the same padding and image size of 300 300 1, we used six blocks of replicated 2D convolutional layers. All convolutional layers had the same kernel size. Still, filters ranging from 4 to 128 pixels in size were employed to extract complex and multi-scale information, creating a feature map from which these characteristics could be sent to other layers and utilized to extract more complicated features.

The filters that make up a CNN's architecture are responsible for learning different aspects of an image: initially, its edges, then its complicated forms, and last, its colours and finer details. CNN design caters for the computational capacity of the input layer by lowering the dimensionality of the input form via max pooling. Additionally, the sizes of each convolutional layer's filter change.

IV EXPERIMENTAL RESULTS AND DISCUSSION

The suggested model was built using Python programming using version 3.8. The experimental results are shown in this chapter. Deep neural networks ResNet50 and Alexnet have been used for training and testing. The results of the model's training and testing are shown in Table 1.

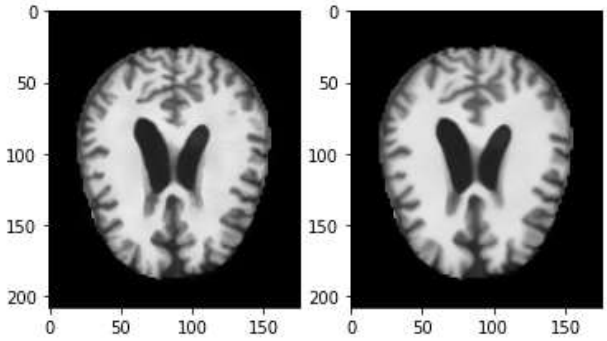

Figure 8: Image Noise Removal using MLP with CNN

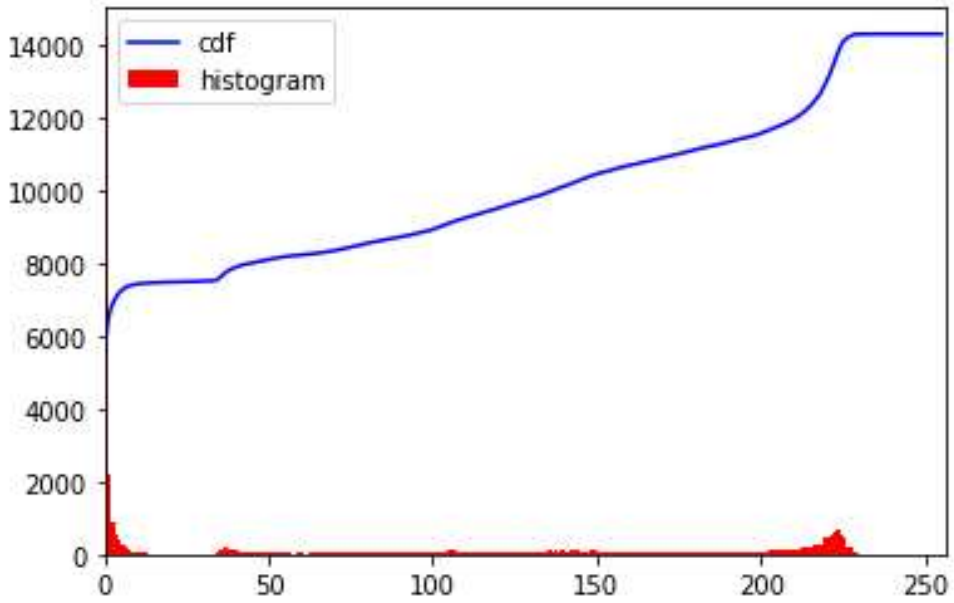

Figure 9: Histogram equalization using the CDF function

The MRI images are noise removed using MLP Algorithm, and the results are illustrated in figure 8. And the histogram equalization done with Cumulative Density Function (CDF) is represented in figure 9.

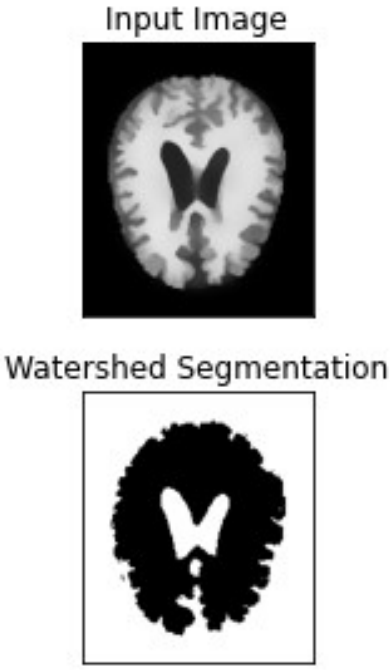

Figure 10: Image Segmentation

Table 1: Training and evaluating values based on the 10 Epoch

Epoch	Training Loss	Validation Loss	Training Accuracy	Testing Accuracy
1	00.1538	00.0637	00.9545	00.9799
2	00.0550	00.0479	00.9830	00.9834
3	00.0354	: 0.0459	00.9894	00.9837
4	00.0248	00.0440	00.9919	00.9871
5	00.0167	00.0478	00.9944	00.9857
6	00.0121	00.0523	00.9957	00.9853
7	00.0080	00.0550	00.9974	00.9857
8	00.0071	00.0567	00.9977	00.9855
9	00.0051	00.0486	00.9983	00.9869
10	00.0066	00.0617	00.9977	00.9853

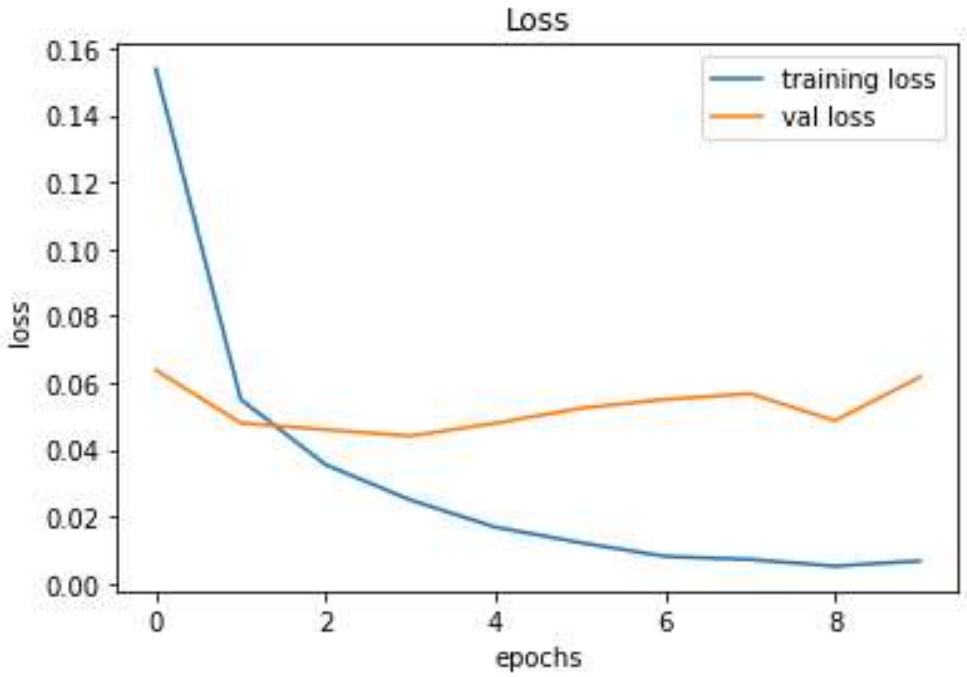

Figure 11: Training and testing loss

As illustrated in Figure 11, the suggested model is trained using loss values. The X-axis represents the Epoch, and the Y-axis represents the lost Value.

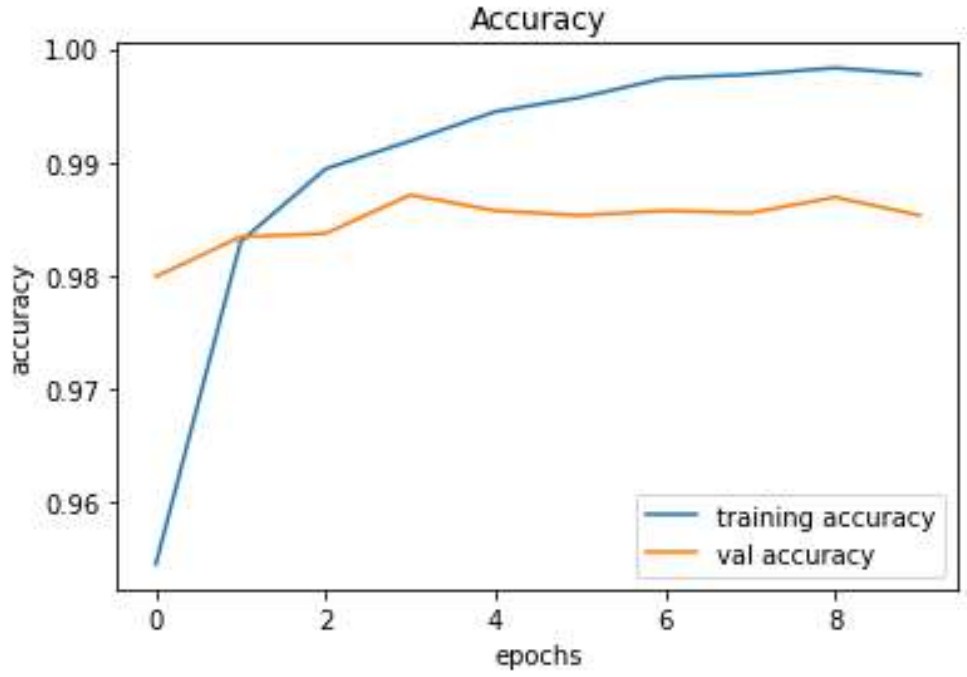

Fig 12: Training and testing Accuracy.

The CNN-ResNet has been trained using 10 Training Epochs, and Figure 12 displays the testing accuracy. The Y-axis reflects the accuracy, while the X-axis represents the Epoch number.

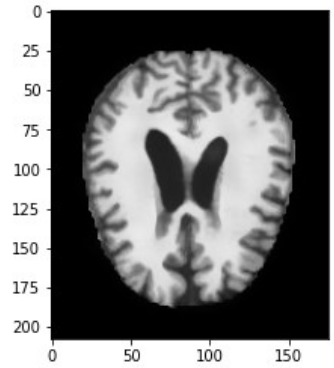

Figure 13: Input MRI Image will be predicted by Moderate Demented

The input MRI image predicted using the proposed model with Moderate Demented output is shown in figure 13.

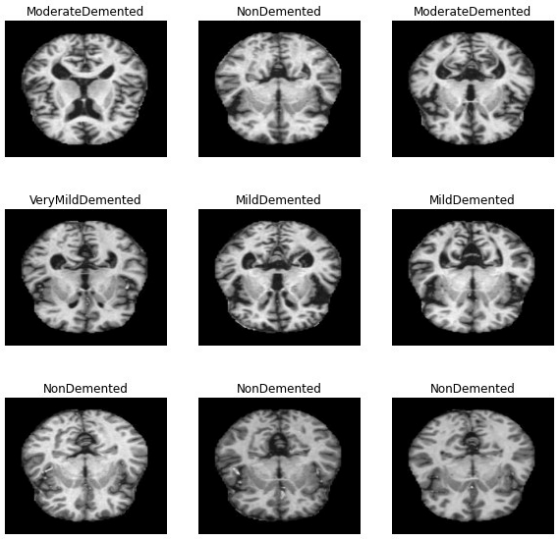

Figure 14: CNN Image Classification

The proposed model achieves 98% accuracy. And the CNN has classified the MRI image as multi-class classification, as shown in figure 14.

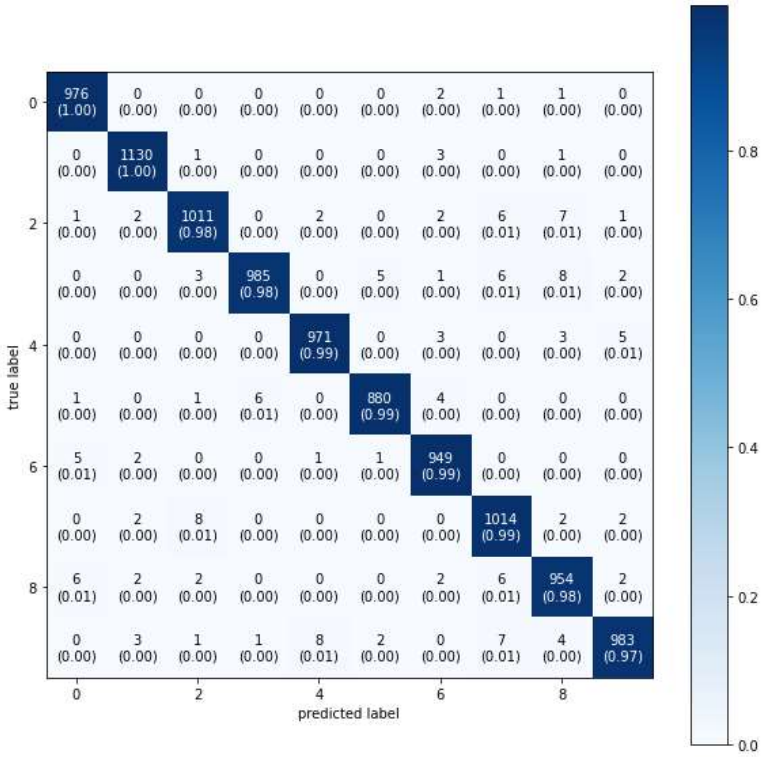

Figure 15: Confusion matrix

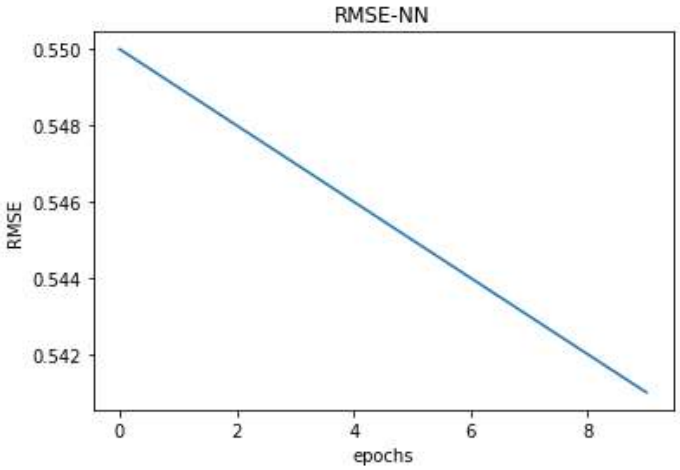

Figure 16: RMSE Value

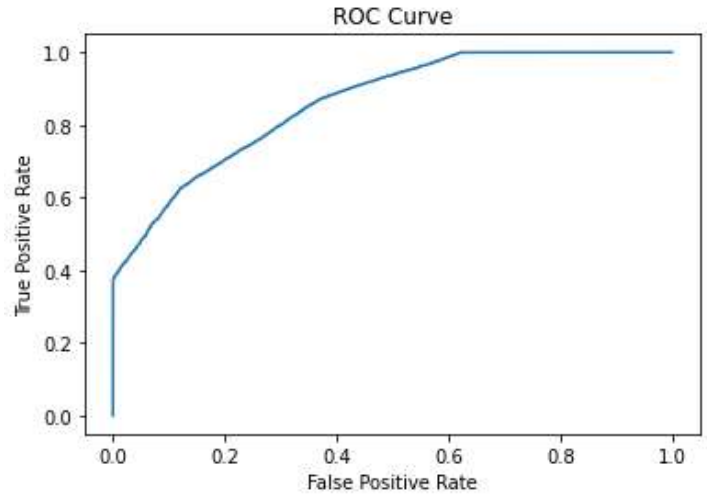

Figure 17: ROC Curve

The prediction overall confusion matrix is shown in figure 15. The RMSE Value is represented in figure 16. The ROC curve is represented in figure 17.

V. CONCLUSION

This study reported on detecting Alzheimer's disease (AD) using a deep learning model, which assists clinicians in the diagnostic process. This research paper has proposed an AD-TL framework for predicting AD as early as. Vascular enlargement and brain atrophy Image segmentation are used to identify more giant Vascular/tumours. The degree of enlargement defines whether a patient is healthy, in the initial stage of Alzheimer's, in the second stage of Alzheimer's, or has moderate cognitive impairment. Brain shrinkage is another crucial element of Alzheimer's disease diagnosis. This research presented a paradigm for the identification of AD at an early stage. The MRI Image noises were removed using MLP with CNN, and the image segmentation was done with watershed image segmentation. The training has been done with Resnet50 with Alexnet architecture. The classification has been done with DCNN. The research reveals that the use of improves classification accuracy. This solves the challenge of early detection while causing no brain injury, and the proposed approach achieves 99% accuracy. This will help to advance medical imaging studies—the future scope of this study is to enhance the authentic MRI images to integrate mobile applications.

VI REFERENCE

1. A.Raj, S. Bujare, A. Gorthi, J. Malik, A. Das and A. Kumar, "Alzheimer's Disease Recognition using CNN Model with EfficientNetV2," 2022 2nd Asian Conference on Innovation in Technology (ASIANCON), 2022, pp. 1-5, doi: 10.1109/ASIANCON55314.2022.9908834.
2. Andersen, E., Casteigne, B., Chapman, W. D., Creed, A., Foster, F., Lapins, A., … Sawyer, R. P. (2021). Diagnostic biomarkers in Alzheimer's disease. Biomarkers in Neuropsychiatry, 5, 100041. doi:10.1016/j.bionps.2021.100041
3. B. Shi, Z. Wang and J. Liu, "Distance-informed metric learning for Alzheimer's disease staging," 2014 36th Annual International Conference of the IEEE Engineering in Medicine and Biology Society, 2014, pp. 934-937, doi: 10.1109/EMBC.2014.6943745.

4. B. T. Padovese, D. H. P. Salvadeo and D. C. G. Pedronette, "Diagnostic Support for Alzheimer's Disease through Feature-Based Brain MRI Retrieval and Unsupervised Distance Learning," 2016 IEEE 16th International Conference on Bioinformatics and Bioengineering (BIBE), 2016, pp. 242-249, doi: 10.1109/BIBE.2016.52.
5. C. A. Ortiz Toro, N. Gutiérrez Sánchez, C. Gonzalo-Martín, R. Garrido García, A. Rodriguez González and E. Menasalvas Ruiz, "Radiomics Textural Features Extracted from Subcortical Structures of Grey Matter Probability for Alzheimer's Disease Detection," 2019 IEEE 32nd International Symposium on Computer-Based Medical Systems (CBMS), 2019, pp. 391-397, doi: 10.1109/CBMS.2019.00084.
6. E. Bicacro, M. Silveira and J. S. Marques, "Alternative feature extraction methods in 3D brain image-based diagnosis of Alzheimer's Disease," 2012 19th IEEE International Conference on Image Processing, 2012, pp. 1237-1240, doi: 10.1109/ICIP.2012.6467090.
7. Haussmann, R., Noppes, F., Brandt, M. D., Bauer, M., & Donix, M. (2021). Lithium: A therapeutic option in Alzheimer's disease and its prodromal stages? Neuroscience Letters, 760, 136044. doi:10.1016/j.neulet.2021.136044
8. M. Mahyoub, M. Randles, T. Baker and P. Yang, "Comparison Analysis of Machine Learning Algorithms to Rank Alzheimer's Disease Risk Factors by Importance," 2018 11th International Conference on Developments in eSystems Engineering (DeSE), 2018, pp. 1-11, doi: 10.1109/DeSE.2018.00008.
9. N. A. Vats, P. Barche, G. S. Mirishkar and A. K. Vuppala, "Exploring High Spectro-Temporal Resolution for Alzheimer's Dementia Detection," 2022 IEEE International Conference on Signal Processing and Communications (SPCOM), 2022, pp. 1-5, doi: 10.1109/SPCOM55316.2022.9840847.
10. Q. Zhou et al., "An Optimal Decisional Space for the Classification of Alzheimer's Disease and Mild Cognitive Impairment," in IEEE Transactions on Biomedical Engineering, vol. 61, no. 8, pp. 2245-2253, Aug. 2014, doi: 10.1109/TBME.2014.2310709.
11. R. Patel, J. Liu, Kewei Chen, E. Reiman, G. Alexander and Jieping Ye, "Sparse Inverse Covariance Analysis of the human brain for Alzheimer's disease study," 2009 ICME International Conference on Complex Medical Engineering, 2009, pp. 1-5, doi: 10.1109/ICCME.2009.4906604.
12. Rapaka, D., Bitra, V. R., Challa, S. R., & Adiukwu, P. C. (2021). Potentiation of microglial endocannabinoid signalling alleviates neuroinflammation in Alzheimer's disease. Neuropeptides, 90, 102196. doi:10.1016/j.npep.2021.102196
13. Teipel, S. J., Dyrba, M., Chiesa, P. A., Sakr, F., Jelistratova, I., Lista, S., … Grothe, M. J. (2020). In vivo staging of regional amyloid deposition predicts functional conversion in the preclinical and prodromal phases of Alzheimer's disease. Neurobiology of Aging, 93, 98–108. doi:10.1016/j.neurobiolaging.2020.03.011
14. Wei, X., Du, P., & Zhao, Z. (2021). Impacts of DNA methylation on Tau protein-related genes in the brains of patients with Alzheimer's disease. Neuroscience Letters, 763, 136196. doi:10.1016/j.neulet.2021.136196